Table 1 Summarized product data of T 55% AS4 / PES-4100 0.14 x 25.4

Tape designation	T55% AS4/PES-4100
Carbon fibers	Hexcel HS-CP-5000-AS4
Fiber volume fraction	55% ± 3.00%
Matrix material	Sumitomo Sumikaexcel Polyethersulfone 4100 MP (PES)
Tape width	25.375 ± 3.00%
Tape thickness	0.1372 mm ± 5.00%

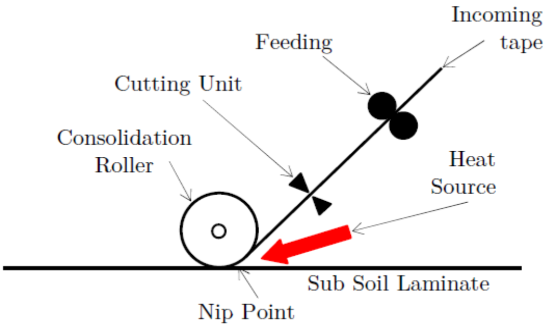

Figure 1 Schematic of the AFP process for composites with thermoplastic matrix [13]

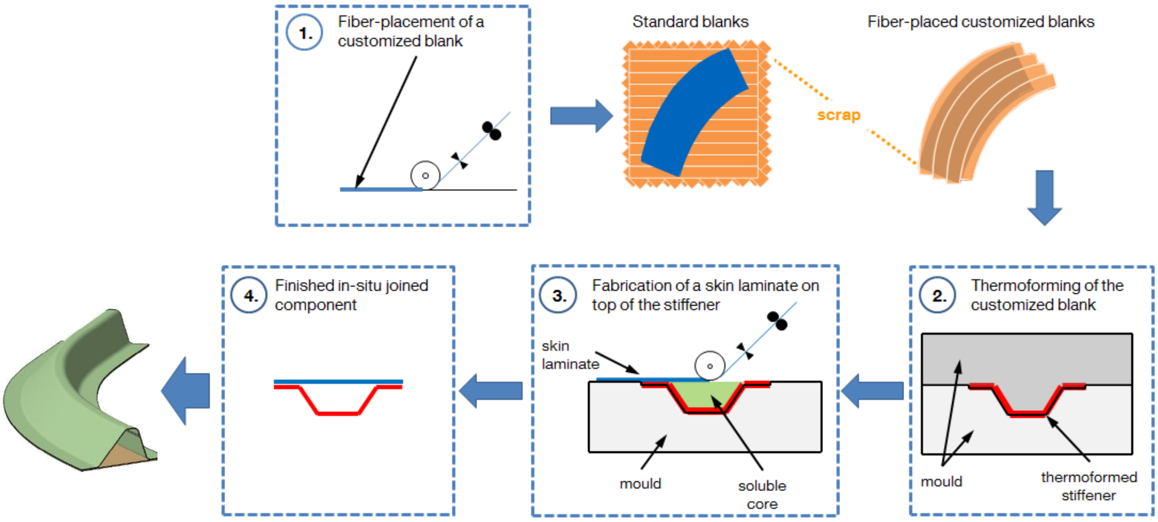

Figure 2 Flow-chart of the DEfcodoor production concept

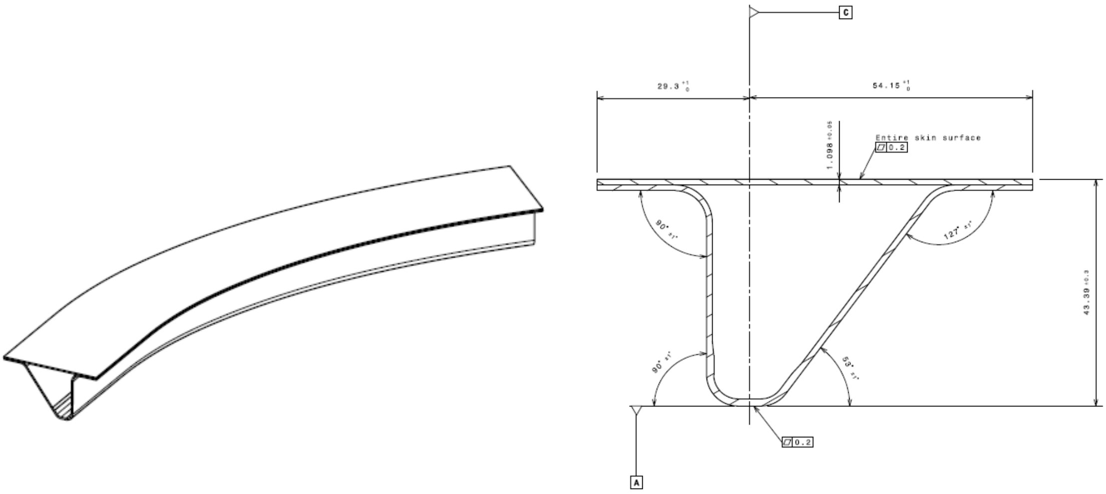

Figure 3 Feasibility Article DEfcodoor Project

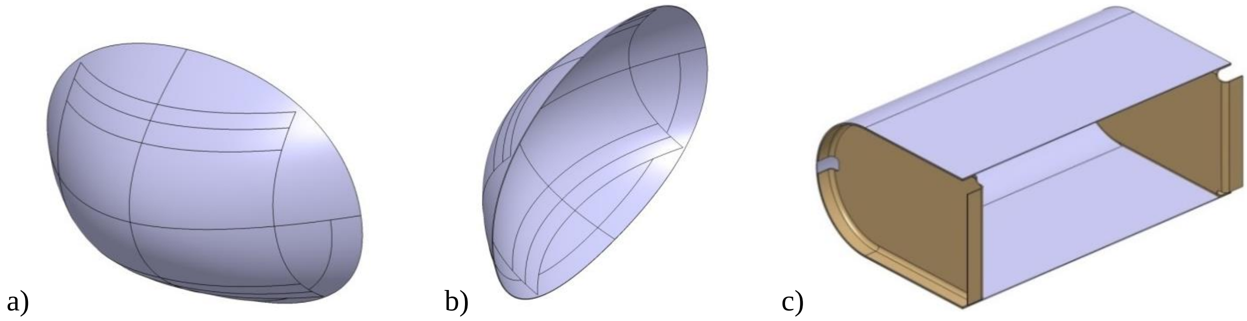
a)
b)
c)

Figure 4 Planed demonstrators for the GRC6.2 Project (ECO-Fairs): a) and b) Radom; c) sponson fairing (AW)

Table 2 Welding and thermal properties of PES and PPS

		DEfcodoor	**ECO-Fairs**
Polymer Type		**PES** *Polyesthersulfone*	**PPS** *Polyphenylenesulfide*
Microstructure		Non-crystalline (amorphous)	Semi-crystalline
T_g		215°C	85°C
T_m		-	285°C
Long-term Heat Resistance		160 – 200°C	200 – 240°C
Water absorption		Partially	Very low
Possible welding partners	Structural	PEEK, PSU	-
	Adhesive	PBT, PET, PC, PA66	PA66

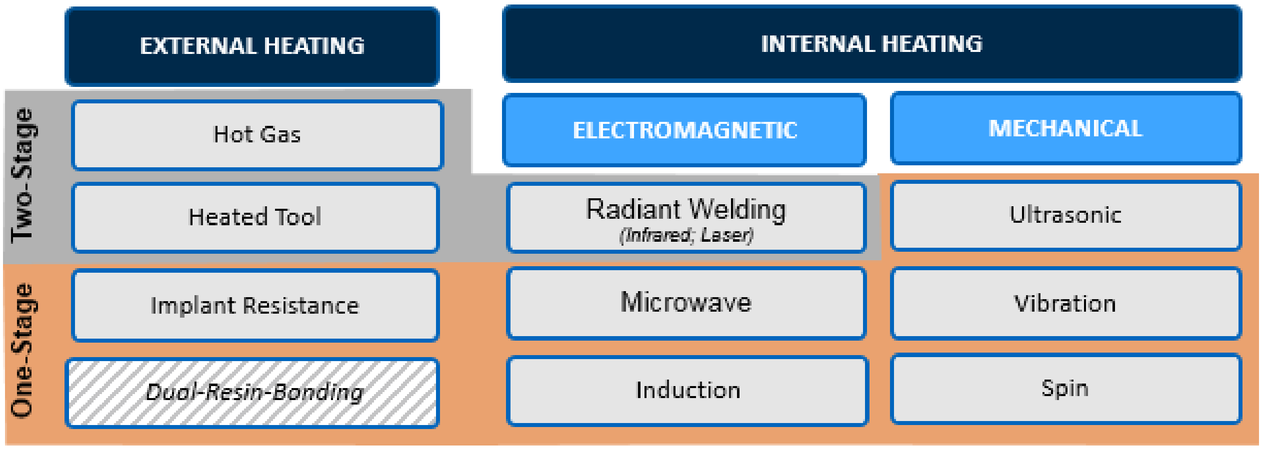

Figure 5 Classification of different welding methods for TPCs

o	*Not suitable for the disassembly of TPCs*
+	*Only adaptable for the disassembly of TPCs under high research effort*
++	*Adaptable under medium research effort*
+++	*Good suitability for the disassembly of TPC structures, with low or no research effort*

Table 3 Benchmark overview of separation scenarios from literature

Heating / Welding Method		Evaluation
Bulk heating	Co-consolidation	o
	Hot-melt-thermoplastics	o
	Dual-resin bonding	++
Frictional heating	Spin and vibration welding	o
	Ultrasonic welding	o
Thermal heating	Hot-tool welding	o
	Hot-gas welding	o
	Infrared welding	o
	Laser welding	+
Electromagnetic heating	Dielectric welding	+
	Microwave	+
	Resistance welding	+++
	Inductive welding	+++

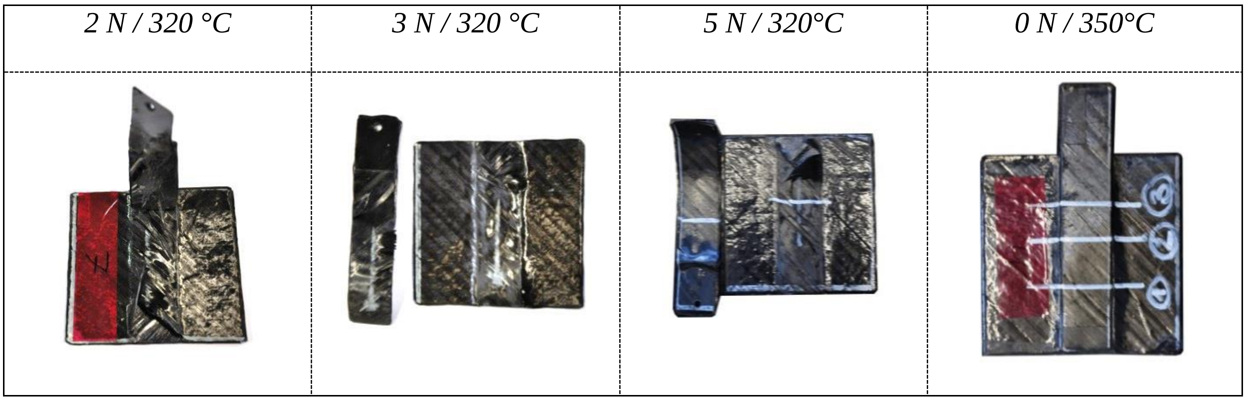

2 N / 320 °C

3 N / 320 °C

5 N / 320°C

0 N / 350°C

Figure 6 Selection of separated coupons by means of inductive heating

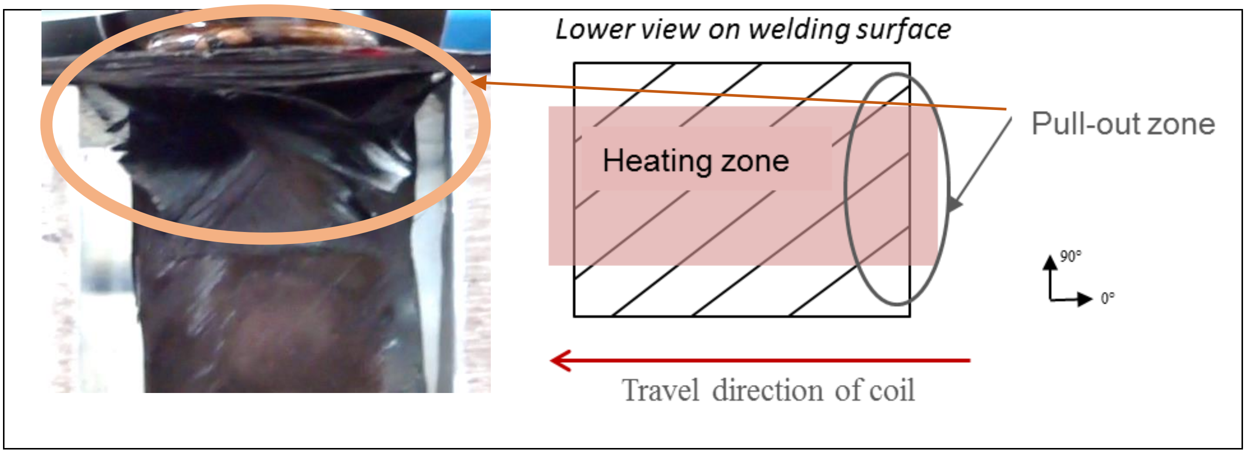

Figure 7 Schematic of the pull-out effect of fiber tows at the edge of the heating region for 45° plies

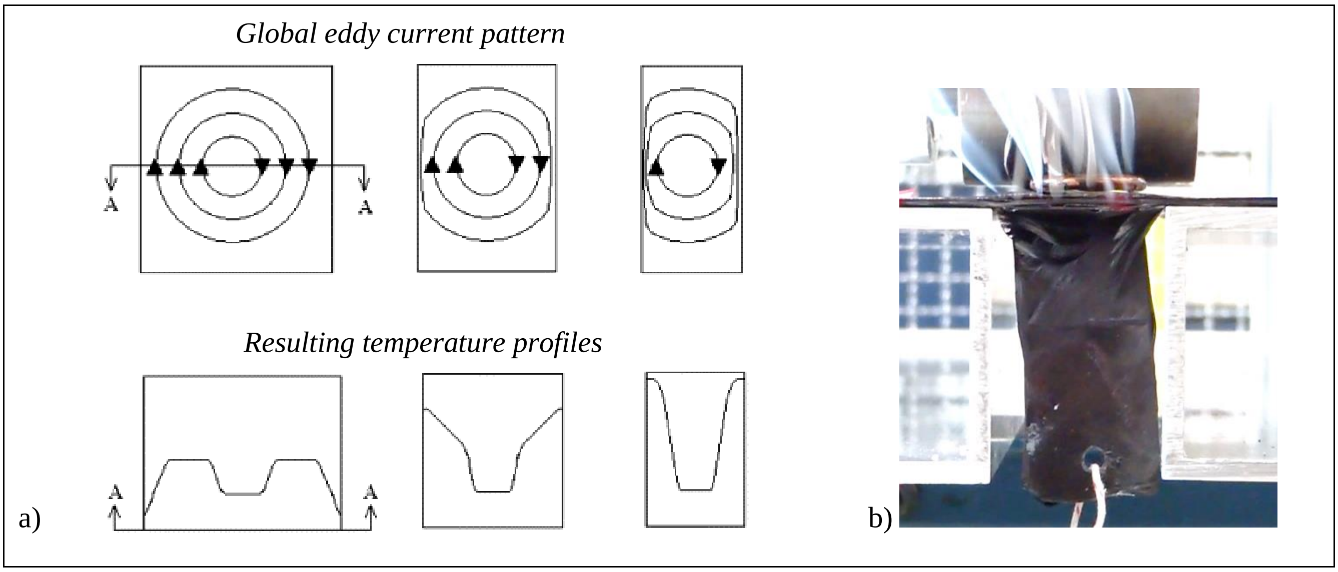

Figure 8 a) Edge effect as a result of changing geometry; b) Matrix deterioration as a result of the edge effect

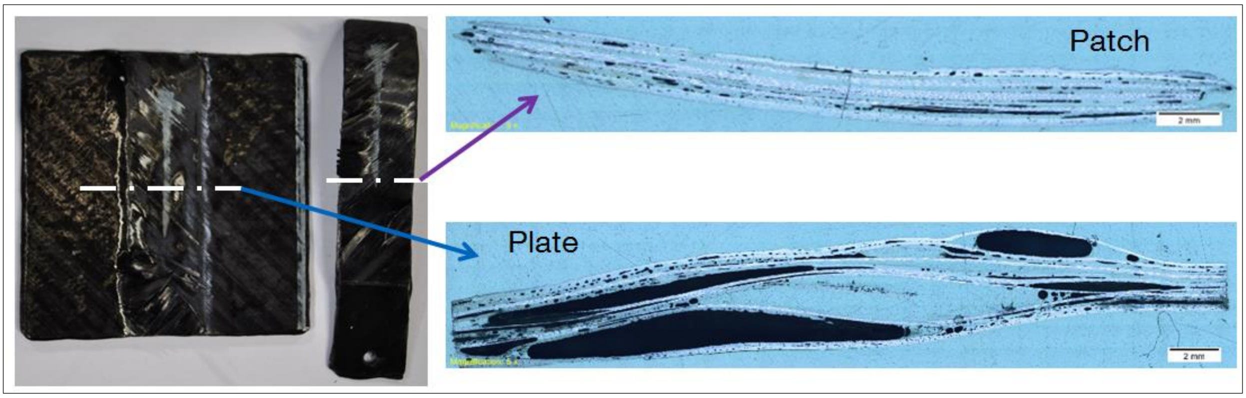

Figure 9 Micrograph of disassembled coupon: Plate is delaminated, patch remains consolidated

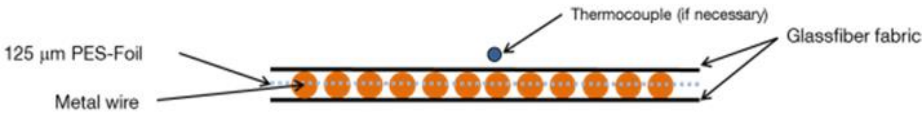

Figure 10 Conceptual layup of the separation layer with minimum insulation layer (glass fiber fabric)

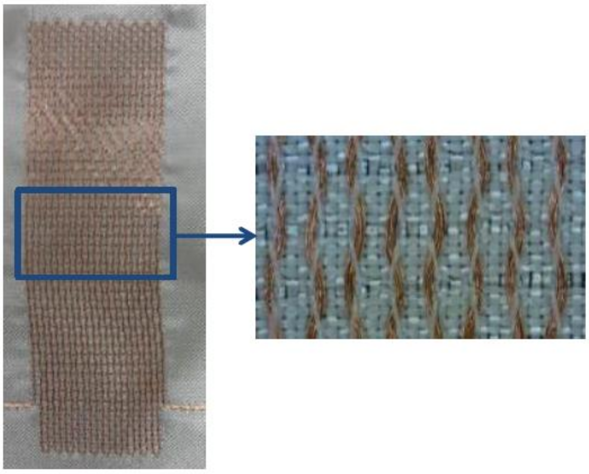

Figure 11 Stitching pattern of resistive implant

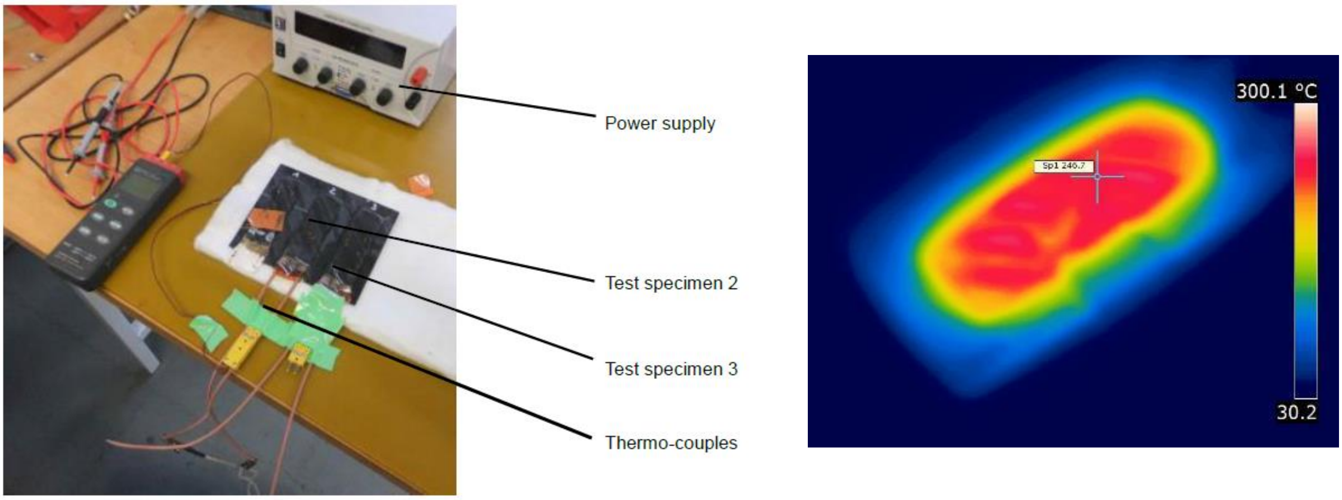

Figure 12 right: Test set up for disassembly trials on coupon level; left: exemplary thermography image

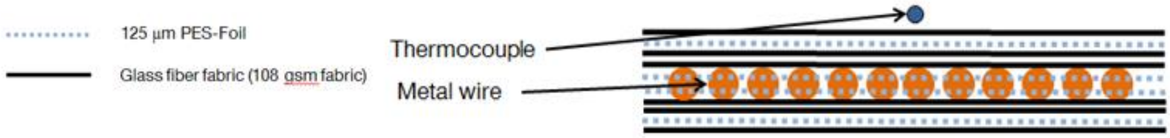

Figure 13 Final layup of separation layer

Figure 14 Light optical micrographs of the embedded final design of the separation layer

$$P = \frac{U^2}{R} \qquad \text{Eq. 1}$$

$$R_1 = R_{ref} \cdot \left[1 + \alpha_{ref} (T_1 - T_{ref})\right] \qquad \text{Eq. 2}$$

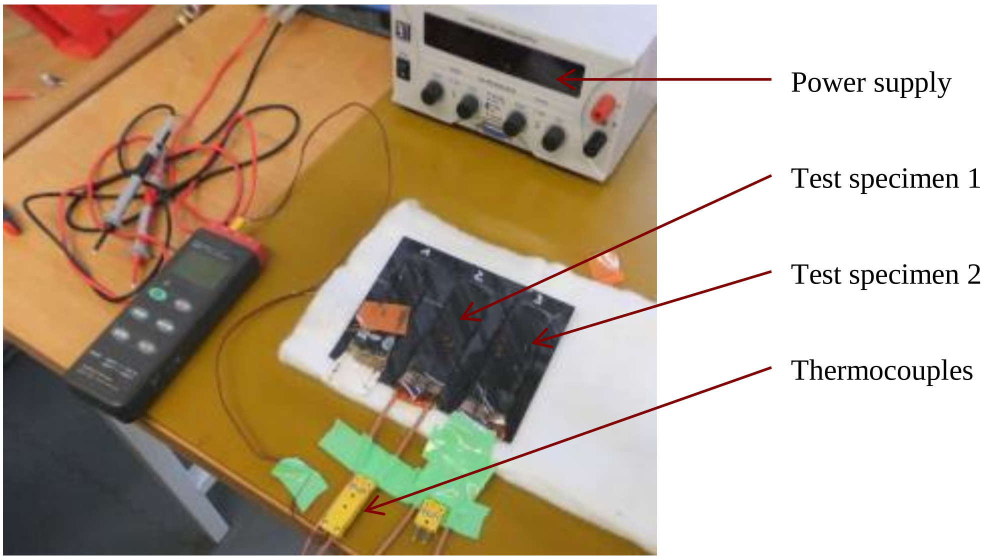

Figure 15 Test set up for disassembly trials

a b c

Figure 16 Picture of test specimen 2 (a) and test specimen 3 (b) after separation test. Exemplary thermographic image of disassembly coupon (c)

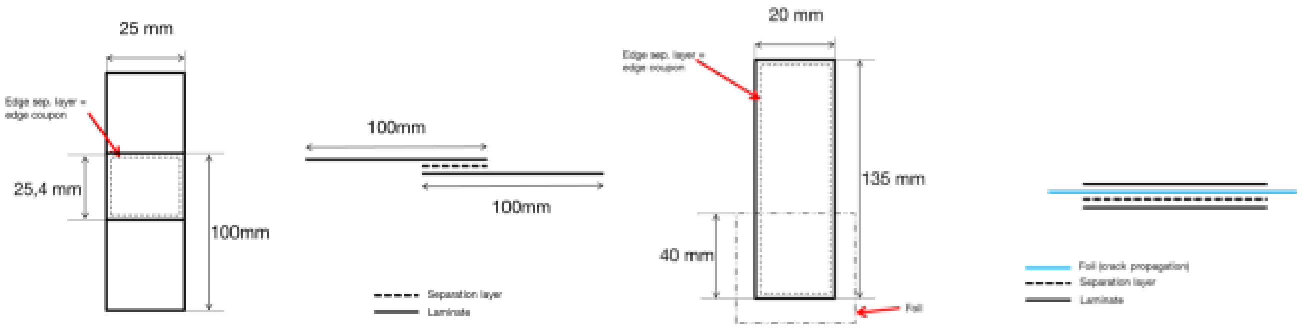

Figure 17 Single lap shear and G1c test specimens

Figure 18 Side view of single lap shear test specimen (without separation layer) with tape undulation

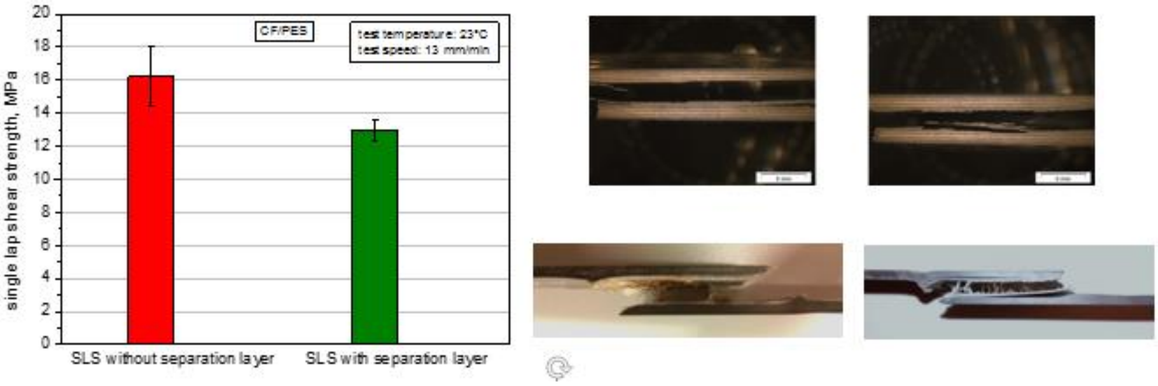

Figure 19 SLS Test Results

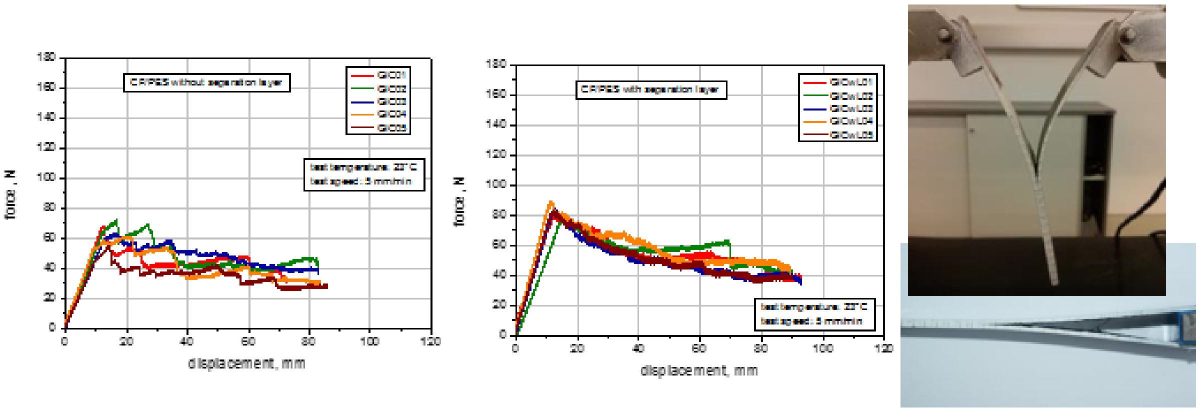

Figure 20 G1c fracture mechanics tests

$$R_{tot} = \frac{1}{\sum \frac{1}{R_i}} = \frac{1}{\frac{1}{R_1} + \frac{1}{R_2}} \qquad \text{Eq. 3}$$

Table 4 Discrete power levels during the disassembly trial on demonstrator level with correspondent calculated values.

Measured Values		*Calculated Values*		
U (V)	**T (°C)**	**R(T) (Ω)**	**P_{ru} (W)**	**I_{calc} (A)**
8,9	65	2	8,42	2,05
6,8	115	2,33	19,86	2,92
Inclusion of insulation layer (at approx.. 172/179°C)				
10,8	225	3,06	38,16	3,53
13,7	300	3,55	52,82	3,86

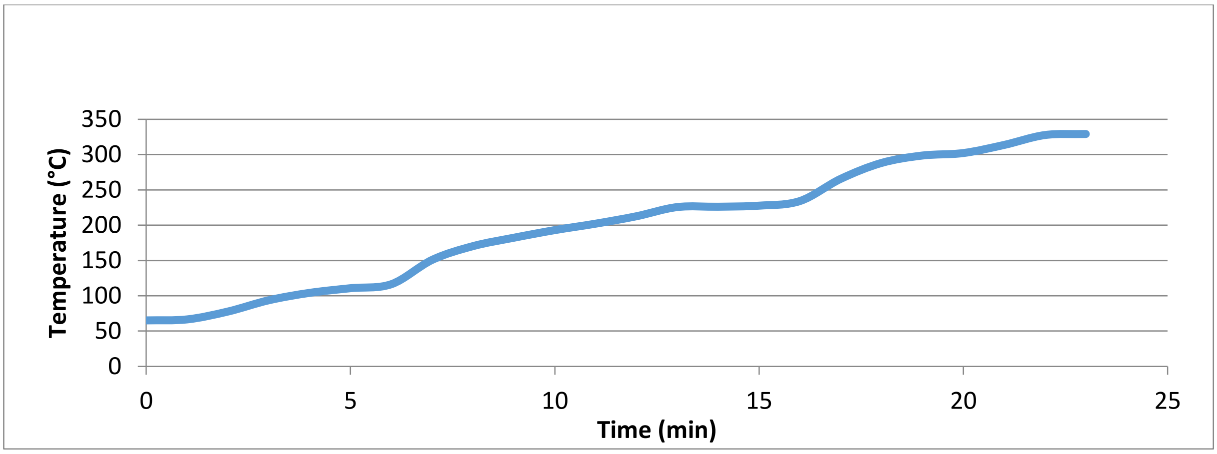

Figure 21 Heating ramp for the disassembly test on demonstrator level (average values)

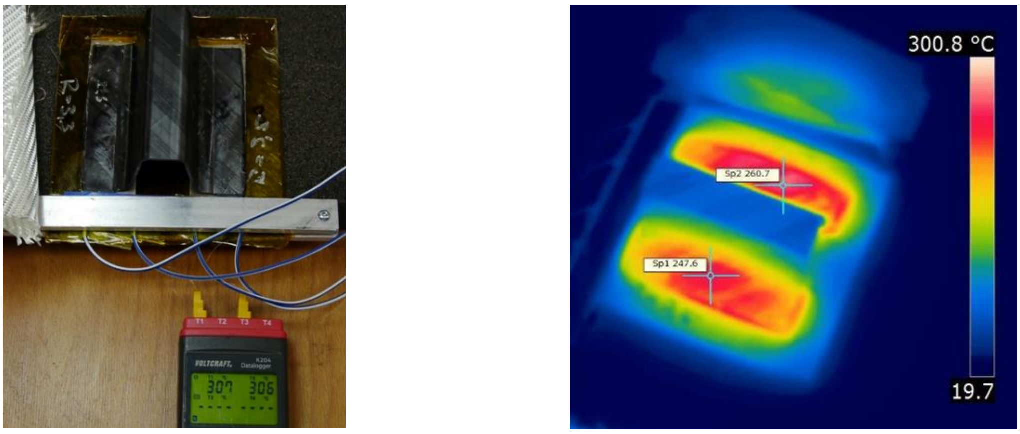

Figure 22 Exemplary picture and thermographic image of the conducted test at approx. 305°C.

Figure 23 Disassembled omega stringer from skin